 DOI: 10.1002/masy.201050406

Ionic Conductivity in Solutions of Poly(ethylene oxide) and Lithium Perchlorate

Noor Hidaya Abdul Nasir, Chin Han Chan, Hans-Werner Kammer, Lai Har Sim, Muhd Zu Azahan Yahya*

Summary: Solution casting technique served to prepare solid solutions of lithium perchlorate and poly(ethylene oxide) (PEO) having different molecular masses. Salt concentrations of solutions were varied between around 2 and 13 wt%. Crystallinity and melting point depression served to determine composition and content of amorphous phase as well as thermodynamic behavior of the solutions. Conductivity as a function of salt concentration in the amorphous phase follows a power law at constant temperature (30 °C). It results that both exponent and mobility of charge carriers increase with ascending molecular mass of PEO. The mobility follows an increase with molecular mass proportional to $M^{2.8}$ indicating dependence of mobility on interstitial volume between chain molecules. Deviation of solution from perfect behavior can be evaluated by melting point depression. Accordingly, increase in conductivity is preferably related to approach to perfect solution behavior. Determination of dielectric function allows some conclusion about ion pair formation in the systems under discussion. It turns out that probability of ion pair formation decreases with increasing molecular mass of PEO in agreement with thermodynamic behavior of the solutions.

Keywords: dielectric function; ionic conductivity; $LiClO_4$; PEO; solid solutions

Introduction

Polymer electrolytes formed by polymer-salt solutions attracted a great deal of scientific interest in the past.[1–8] It is related to the hope for applying these systems in new generations of highly efficient batteries. Preferably used constituents are poly(ethylene oxide) (PEO) and lithium salts.[9–19] The widely accepted idea is that lithium salts are molecularly dispersed in amorphous regions of the polymer. Dissolution of the salt is accompanied by solvation of cations by monomer units of the chain molecules. The coordination sphere of the cation may also comprise the associated anion. Properties of those solutions are essentially coined by developing phase morphologies. Constituents are miscible in the molten state, but display immiscibility in the solid state. Below the melting temperature of PEO, one observes phase separation in pure crystalline PEO and an amorphous phase of PEO and salt. Development of these phases is ruled by competition of two rate processes, the rate of phase separation and the rate of crystallization. At sufficiently high temperatures, close to the melting temperature of the polymer, the rate of crystallization is low and the rate of phase separation is high. Hence, one observes morphologies close to equilibrium. The opposite situation occurs at low temperatures. A high rate of crystallization and a low rate of phase separation lead to non-equilibrium morphologies or freezing in of molten mixtures owing to high viscosity of the mixture. Apart from these morphology developments that influence the homogeneity of salt distribution in

Faculty of Applied Sciences, Universiti Teknologi MARA, 40450 Shah Alam, Malaysia
E-mail: cchan@salam.uitm.edu.my

the polymer, conductivity in solid polymer electrolytes and thermodynamic behavior of these systems are in general a function of ion concentration, molecular mass of the polymer and external conditions. Efforts for improvements of polymer-salt solutions pointed preferably towards two closely related directions, enhancement of both carrier density and mobility.

It becomes evident that interrelations between ions and polymer chains play an important role in conductivity mechanism. We took this into account by a power-law dependence of ionic conductivity σ on salt concentration Y of the amorphous phase, $\sigma = \sigma_o \ (Y)^x$.[20] Exponent x takes into account the extent of correlations between chain segments and salt molecules. This approach should be acceptable as long as the Bjerrum length, l_B, does not exceed the average distance, r, between salt molecules, $l_B/r \leq 1$. We note, this ratio of length scales depends on dielectric constant which itself is a function of salt concentration. In addition to the lengths ratio, which may govern the probability for ion-pair formation, melting point depression provides valuable information about thermodynamic behavior of the solutions under discussion.

Firstly, we briefly sketch the theoretical background. This is followed by experimental results about crystallinity, melting point depression, conductivity and dielectric function. Dependencies on salt content and molecular mass are discussed in terms given in theoretical background.

Experimental Part

Materials

Characteristics of polymers and salt are listed in Table 1. PEO was purified before further use by dissolution in chloroform (Fisher Scientific, Leicestershire, UK) and precipitation in *n*-hexane (Fisher Scientific, Leicestershire, UK) afterwards. The precipitate was filtered off and dried under vacuum. $LiClO_4$ was used after drying in vacuum oven for 48 h at 120 °C.

Sample Preparation

Solution casting technique was used to prepare solid thin films of PEO and $LiClO_4$. Different concentrations of $LiClO_4$ were added to 2% w/w of PEO stock solution in acetonitrile (Fisher Scientific, Leicestershire, UK). The solvent was kept dry by addition of molecular sieves from Merck, Darmstadt, Germany with pore diameter of 3 Å.

The salt concentration was varied in a wide range. It is represented by

$$Y = \frac{\text{mass of } LiClO_4}{\text{mass of PEO}} \quad (1)$$

Polymer films were dried for 24 h at 50 °C before further drying in a vacuum oven for 48 h at the same temperature. Impedance spectroscopy was carried out on the dried polymer films after removing from the vacuum oven. After the impedance analysis, these dried polymer films were stored in desiccators. Approximately 48 h before differential scanning calorimetry (DSC) analysis, samples were dried again in the vacuum oven at 50 °C.

Conductivity Analysis

Ionic conductivity, σ, at 30 °C was determined from ac-impedance measurements using a Hioki 3532-50 Hi-Tester (Nagono, Japan) interfaced with a computer for data acquisition over the frequency range between 100 Hz to 1 MHz. Films of polymer electrolyte were sandwiched between two stainless steel disk electrodes, which acted as blocking electrodes for ions. Quantity σ was calculated from the bulk electrolyte resistance R_b by adopting equation

$$\sigma = \frac{L}{AR_b} \quad (2)$$

Quantities L and A denote thickness of the polymer electrolyte film and its surface area in contact with the stainless steel disk electrodes. Diameter of the electrode is 20 mm. The average of thickness L was determined from three measurements of thickness on the dry polymer film at three different positions that were in contact with the stainless steel disk electrodes.

Table 1.
Characteristics of the PEO samples and lithium perchlorate.

Constituents	PEO_1	PEO_2	PEO_3	$LiClO_4$
M_η[a]/g mol^{-1}	600,000	1,000,000	4,000,000	
T_m[b]/°C	67	67	68	236[e]
T_g[c]/°C	−58	−58	−56	
ΔH_{ref}/J g^{-1}		188.3[d]		272.3[f]
Molecular Structure		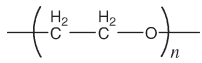		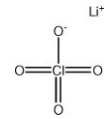
Supplier	Aldrich Chemical Co. (St. Louis, MO)			Acrōs, Organics Co. (Geel, Belgium)

[a]Viscosity-average molecular weight provided by the supplier.
[b]Melting temperature during first heating cycle as determined in this work.
[c]Glass transition temperature after quench cooling as determined in this work.
[d]Melting enthalpy of 100% crystalline PEO from ref. [21].
[e]Melting temperature adopted from ref. [22].
[f]Melting enthalpy adopted from ref. [23].

Thickness was measured by use of Mitutoyo Digimatic Caliper. The thickness of the solid films is in the range of 0.25–0.40 mm. The average of ionic conductivity, σ, was determined after three impedance analysis. The errors for quantities σ are approximately 3%.

Dielectric constant (ε) is calculated from

$$\varepsilon(\omega) = \frac{-\omega B Z''}{(\omega B)^2\left[(Z')^2+(Z'')^2\right]} \quad (3)$$

where Z' and Z'' denote real and imaginary part of impedance that result from ionic conductivity measurements. Quantity B equals $\varepsilon_o A/L$ with L and A as explained above, ω represents the angular frequency and ε_o is the permittivity of free space. Analogously, the dielectric loss (ε'') is given by

$$\varepsilon''(\omega) = \frac{\omega B Z'}{(\omega B)^2\left[(Z')^2+(Z'')^2\right]} \quad (4)$$

Differential Scanning Calorimetry

Perkin-Elmer DSC7 (Shelton, CT), calibrated with indium and zinc standards, has been used for the analysis of samples under nitrogen purge. Sample weights amounted to around 7 mg in DSC experiments. Samples were heated up from 30 to 80 °C with a rate of 20 K min^{-1}. This heating procedure yielded melting temperature and heat of melting for the as-prepared samples.

Theoretical Background

We adopt here the approach to ionic conductivity presented in Ref. [20]. In the range of low salt concentration, the amorphous phase contributes dominantly to conductivity. It is given by

$$\sigma = N_A e \mu^* \alpha^* c_S'' \quad (5)$$

The symbols have the following meaning: N_A – Avogadro number, e – elementary charge, μ^*- ion mobility, α^* - degree of dissociation, c_S'' – molar salt concentration in the amorphous phase. Quantities μ^* and α^* are also functions of salt concentration All concentration dependencies we take into account by a power law in Y. Accordingly, it follows for Eq. (5)

$$\sigma = N_A e \mu \alpha \frac{\rho_P}{M_S}(Y'')^x \quad (6)$$

where Y'' refers also to amorphous phase Exponent x has to be determined experimentally. Quantities μ and α are independent of concentration and ρ_P and M_S represent density of the polymer and

molecular mass of the salt molecule, respectively. Properties of these solutions are strongly governed by interactions between salt molecules and segments occupying the volume r^3 related to the average distance between salt molecules. We take correlations approximately into account by the power law indicated above. For Y it holds true $Y \propto (a/r)^3$ that is it is proportional to the ratio of monomer volume to the volume available to a salt molecule. Exponent x describes the extent of correlations between salt molecules and segments.

Two length scales in the amorphous phase of the polymer electrolyte may rule the behavior of ions: the average distance r between two ions in the amorphous phase and the Bjerrum length l_B, which gives the distance between two charges where Coulomb interaction equals thermal energy. The former quantity can be approximated by

$$r \approx (NA\alpha^* c_S'')^{-1/3}$$

where c_S'' is the molar salt concentration in the amorphous phase and α^* the degree of dissociation. We approximate $\alpha^* c_S''$ by Y'' in the same way as in Eq. (6). It follows

$$r = \left(N_A \frac{\rho_P}{M_S}\right)^{-1/3} (Y'')^{-x/3} \quad (7)$$

In (7), the degree of dissociation $\alpha \approx const$ has been ignored. Bjerrum length reads in usual terms, $l_B = e^2/(4\pi\varepsilon_o \varepsilon k_B T)$. As mentioned previously,[20] this length equals $l_B = 55.13\,\text{nm}/\varepsilon$ at 30 °C. The ratio of these characteristic length scales reads with (7)

$$\frac{l_B}{r} = \frac{55.13\,\text{nm}}{\varepsilon(Y)} \left(N_A \frac{\rho_P}{M_S}\right)^{1/3} (Y'')^{x/3} \quad (8)$$

We note that dielectric constant ε itself is a function of salt concentration. When distance r exceeds Bjerrum length l_B the probability diminishes for ion pair formation. In the opposite case, for $l_B/r > 1$, ion pair formation becomes more likely. Eq. (8) shows that large exponents x and high values of dielectric constant suppress formation of ion pairs.

When PEO and the Li salt are completely miscible in the molten state, we may engage melting point depression of PEO for estimation of deviations from perfect behavior. It is given by

$$T_m = T_m^o + \frac{R(T_m^o)^2}{\Delta H_m} \left[\frac{\ln\gamma_P}{\ln X_P} + 1\right] \ln X_P \quad (9)$$

where X_P represents the mole fraction of polymer in the molten state and γ_P the corresponding activity coefficient. For small salt concentration, we get $\ln X_P = -X_S$. A plot of T_m versus X_S provides information about activity coefficient γ_P. This relationship is valid as long as pure PEO crystallizes out from the molten mixture. We apply Eq. (9) to the as-prepared samples. Therefore, quantities T_m^o and ΔH_m symbolize the melting temperature of pure PEO and the melting enthalpy of fully crystalline polymer; X_S denotes the mole fraction of salt added to the polymer.

Results and Discussion

Crystallinity and Composition of the Amorphous Phase

During preparation, samples undergo phase separation in a pure crystalline phase of PEO and an amorphous mixture of salt and PEO. The extent of phase separation can be evaluated by crystallinity. Therefore, crystallinity was determined for the as-prepared samples as described in Experimental. DSC thermograms for the heating cycle of as-prepared neat PEO_1 and with 13 wt% of salt are presented in Figure 1. The thermograms for as-prepared neat PEO_2 and PEO_3 are not shown due to the overlapping of the respective thermogram with that of the PEO_1. Since only the amorphous phase contains salt or corresponding ions, only this phase guarantees electric conductivity at least in the range of low salt content. Therefore, the composition of the amorphous phase is an essential characteristic of the polymer electrolyte. Degree of crystallinity allows for estimation of the composition of the amorphous phase.

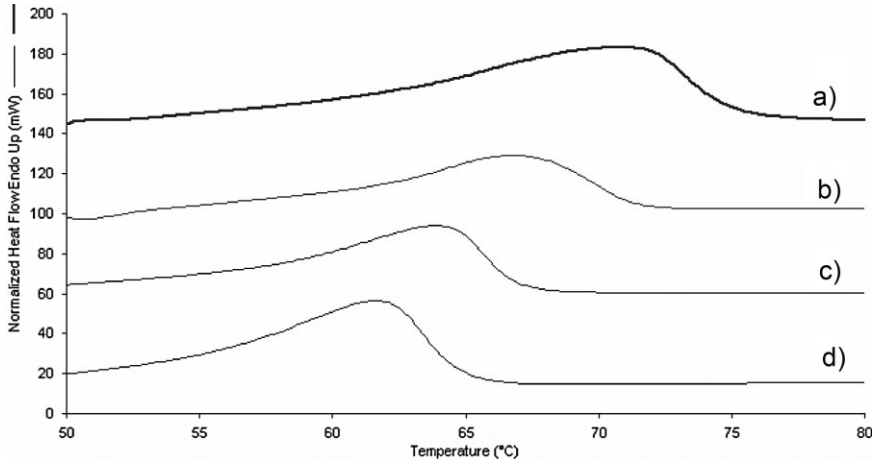

Figure 1.
DSC traces of heating cycles for PEO in as-prepared samples comprising mass fraction of salt, $W_S = 0.13$. The DSC traces are displaced for better identification. (a) neat PEO_1; at $W_S = 0.13$: (b) PEO_1, (c) PEO_2 and (d) PEO_3.

Melting enthalpies, selected values are listed in Table 2, are used to calculate the degree of crystallinity, $X^* = \Delta H_m/\Delta H_m^o$. We apply as reference $\Delta H_m^o = 188.3\,J/g$,[21] the necessary heat for melting of 100% crystalline PEO. Figure 2 shows crystallinity versus salt concentration. We note that for $M = const$ crystallinity of PEO in salt solutions with low salt content stays constant to a good approximation. It does not change significantly with molecular mass. Some scatter occurs at higher salt content. Only for PEO with the highest molecular mass, we observe a slight decrease in crystallinity as compared to samples with lower molecular mass. Moreover, the change of crystallinity with salt content does not depend on molecular mass, $(\partial X^*/\partial W_S)_M = const$.

The mass fraction of salt in the amorphous mixture, W_S'', is related to degree of

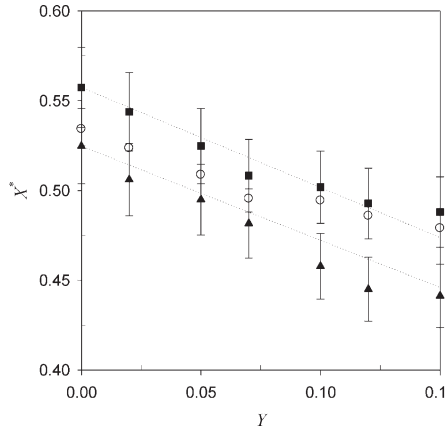

Figure 2.
Crystallinity X^* of PEO in as-prepared samples versus concentration of $LiClO_4$; dotted lines represent loci of constant PEO crystallinity ■ – PEO_1, ○ - PEO_2, ▲ - PEO_3.

Table 2.
Selected melting points (T_m) and melting enthalpies (ΔH_m) for as-prepared samples of PEO/$LiClO_4$ solutions.

Y	PEO_1		PEO_2		PEO_3	
	T_m/°C	ΔH_m/J g^{-1}	T_m/°C	ΔH_m/J g^{-1}	T_m/°C	ΔH_m/J g^{-1}
0	70.8	105.0	70.6	100.6	69.4	98.8
0.05	69.3	98.8	67.1	95.8	66.5	93.2
0.10	67.9	94.5	65.6	93.1	64.8	86.2
0.15	66.7	91.9	64.3	90.2	62.1	83.1

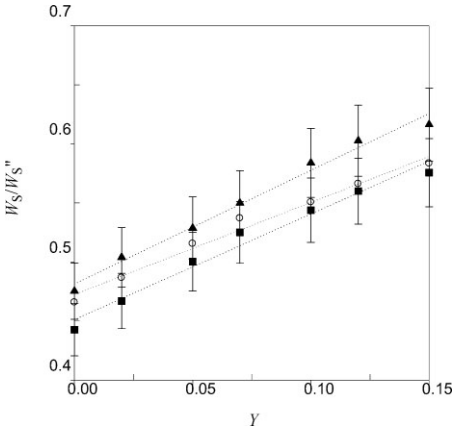

Figure 3.
Mass fraction of the amorphous phase as a function of salt content Y ■ - PEO_1, ○ - PEO_2, ▲ - PEO_3.

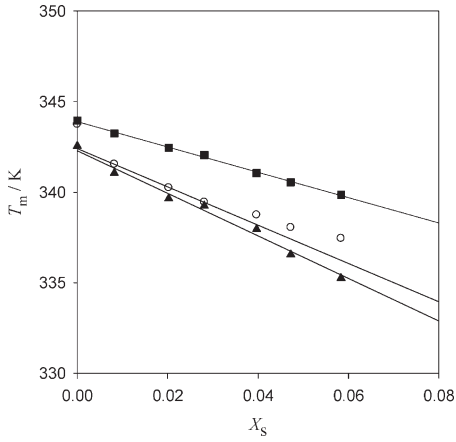

Figure 4.
Melting point of PEO as a function of mole fraction of salt, the solid curves give linear regressions for low salt content ■ - PEO_1, ○ - PEO_2, ▲ - PEO_3.

crystallinity X^* by

$$W_S'' = \frac{W_S}{1 - X^* \cdot W_P} \tag{10}$$

where W_S and W_P refer to the concentration of salt and polymer in the homogeneous system. Eq. (10) does not necessarily represent the equilibrium composition of the amorphous phase. It gives the composition of the amorphous phase in the as-prepared sample. The ratio W_S/W_S'' represents the mass fraction of amorphous phase in the phase separated solution. It is plotted versus salt content Y in Figure 3. In agreement with Figure 2, the mass fraction of amorphous phase does not depend significantly on molecular mass. It varies from around 45% to 60% when the salt content increases from zero to around 13 wt%.

Following Eq. (9), we adopt melting point depression of the as-prepared samples for evaluation of the solid solution. Selected melting points are listed in Table 2.

PEO samples (Figure 4). Results are listed in Table 3. We observe that the solution with PEO_3, the polymer with the highest molecular mass, behaves perfectly to a good approximation whereas the solution comprising PEO_1 displays pronounced deviations from ideality.

Conductivity

We determined conductivities after Eq. (2) and evaluate results according to Eq. (5). A double-logarithmic plot of conductivity versus concentration Y'' yields exponent x and mobility $\alpha\mu$. This is shown in Figure 5 in the concentration range $0.02 \leq Y \leq 0.15$ for salt solutions comprising PEO of different molecular mass at 30 °C. The concentration Y corresponds to mass fraction of salt, W_S, in the range 0.0196 . . .0.1304 and to $0.044 \leq Y'' \leq 0.293$. The following exponential functions are obtained:

$$\begin{aligned}
&PEO_1: \quad \sigma = 4.34 \cdot 10^{-4} (Y'')^{3.08}\ (\Omega\,\mathrm{cm})^{-1}\ \text{(correlation : 0.996)} \\
&PEO_2: \quad \sigma = 7.08 \cdot 10^{-3} (Y'')^{3.87}\ (\Omega\,\mathrm{cm})^{-1}\ \text{(correlation : 0.988)} \\
&PEO_3: \quad \sigma = 0.13 (Y'')^{4.60}\ (\Omega\,\mathrm{cm})^{-1}\ \text{(correlation : 0.987)}
\end{aligned} \tag{11}$$

From data as given in Table 2, one gets melting point depressions, $\Delta T(X_S)$, for the

Mobilities $\alpha\mu$ and exponents x provided by regression functions (11) are listed in

Table 3.
Melting point depressions and activity coefficients from Eq. (9) in the range of low salt concentration.

Polymer	Melting point depression from (9) (correlation)	Activity coefficient γ_P
PEO_1	$\Delta T/K = 70.1.\ X_S$ (0.999)	$1 + 0.409X_S$
PEO_2	$\Delta T/K = 105.7.\ X_S$ (0.9999)	$1 + 0.102X_S$
PEO_3	$\Delta T/K = 117.4.\ X_S$ (0.979)	$1 + 0.002X_S$

Table 4. Molecular characteristics adopted for determination of quantity $\alpha\mu$ are $M_S = 106.5$g mol^{-1}, $M_{monomer} = 44$ g mol^{-1} and $\rho_P = 1.2$ g cm^{-3}.

Data of Table 4 demonstrate that both mobility and exponent x increase with molecular mass of the polymer. Increasing exponent means after Eq. (7) that the number of chain segments involved in solvation of salt molecules increases with molecular mass. Perfect thermodynamic behavior of solutions with PEO_3 eases transport of charge carriers. A plot of mobility as a function of molecular mass at 30 °C leads to the following interesting result

$$\alpha\mu = K_\mu M_\eta^{2.8} \tag{12}$$

with $K_\mu = const$ for the system under discussion. The exponent is close to three. Hence, mobility is proportional to the interstitial volume between chains (R_{int}^3) with R_{int} being proportional to degree of polymerization N.

Adopting Nernst's relationship, one may relate mobility $\alpha\mu$ to diffusion coefficient of the charge carriers. It follows

$$D = \frac{k_B T \alpha\mu}{e} \tag{13}$$

Data in Table 4 show that the diffusion coefficient increases in PEO_3 by two orders of magnitude as compared to PEO_1.

The Dielectric Function

The ratio l_B/r provides some information about the probability of ion-pair formation in the system. This requires, however, knowledge about the function ε (Y) after

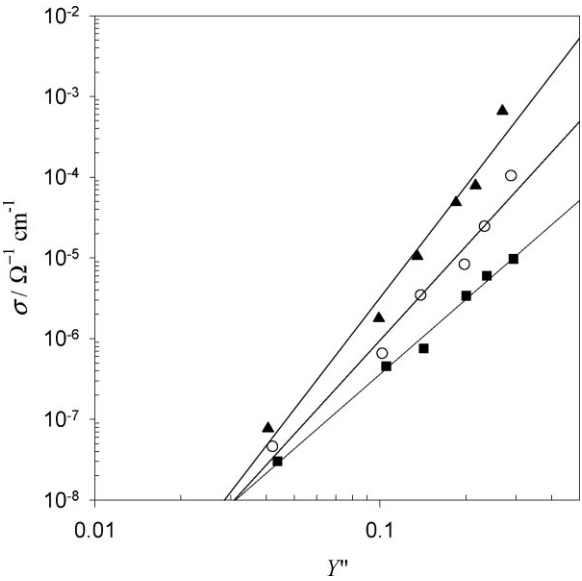

Figure 5.
Conductivity versus salt content Y'' of the amorphous phase in PEO/$LiClO_4$ solutions at 30 °C; ■ – PEO_1, ○ - PEO_2, ▲ - PEO_3

Table 4.
Mobilities $\alpha\mu$, exponents x and diffusion coefficients from Eq. (13) for PEO/$LiClO_4$ solutions.

Polymer	$M_\eta \cdot 10^{-5}$/g mol^{-1}	$\alpha\mu$/(cm^2 V^{-1} s^{-1})	x	D/cm^2 s^{-1}
PEO_1	6	$4.0 \cdot 10^{-7}$	3.08	$1.0 \cdot 10^{-8}$
PEO_2	10	$6.5 \cdot 10^{-6}$	3.87	$1.7 \cdot 10^{-7}$
PEO_3	40	$1.2 \cdot 10^{-4}$	4.60	$3.1 \cdot 10^{-6}$

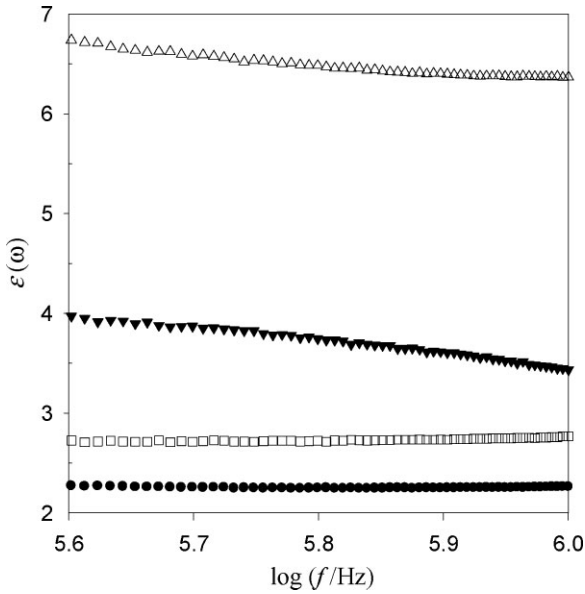

Figure 6.
Dielectric constant versus frequency for different concentrations of $LiClO_4$ in PEO_1 at 30 °C; Y = ● - 0, □ - 0.02, ▼ - 0.07, Δ - 0.12

Eq. (8). Figure 6 presents the dielectric constant as a function of frequency for PEO_1/$LiClO_4$ solutions at 30 °C. Selected data are compiled in Table 5. It turns out that the dielectric constant increases with molecular mass. This tendency becomes more pronounced with ascending salt content.

We apply the dielectric data in Eq. (8) for calculation of the ratio l_B/r as a function of concentration Y''. This is shown in Figure 7. After Eq. (8), the ratio decreases with increasing exponent x and dielectric constant ε. Accordingly, the probability for ion pair formation descends with increasing molecular mass of PEO. This is in qualitative agreement with the thermodynamic behavior given in Table 3.

Table 5.
Dielectric constant ε for solutions of PEO and $LiClO_4$ at 30 °C and frequency $8 \cdot 10^5$ Hz.

Y	PEO_1	PEO_2	PEO_3
0.02	2.74	2.76	2.86
0.05	2.98	5.16	5.24
0.10	4.92	7.38	7.98
0.12	6.40	9.98	15.68

In addition to real parts of dielectric function also dielectric losses were determined for the polymers and for different concentrations of salt (Figure 8). Selected data are listed in Table 6.

Using data as listed in Tables 6 and 7, we calculate the dissipation factor

$$DF = \frac{\varepsilon''}{\varepsilon} \tag{14}$$

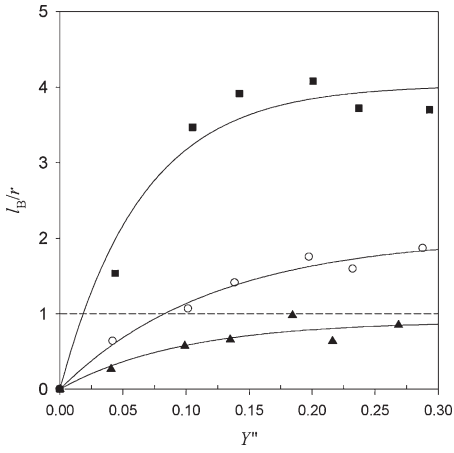

Figure 7.
Ratio of length scales as a function of concentration Y'' after Eq. (8); ■ - PEO_1, ○ - PEO_2, ▲ - PEO_3

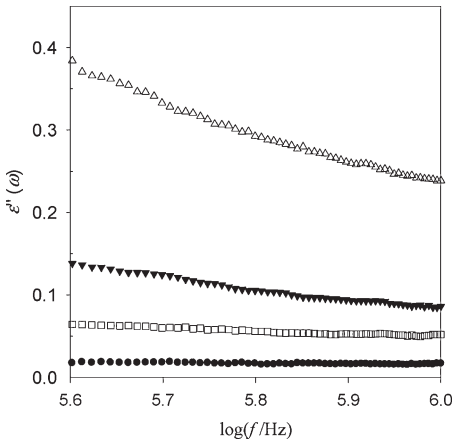

Figure 8.
Dielectric loss of $PEO_1/LiClO_4$ solutions at 30 °C as a function of frequency for different salt concentrations Y; Y = ● - 0, □ - 0.02, ▼ - 0.07, Δ - 0.12

Table 6.
Dielectric loss ε'' for different salt concentrations at 30 °C and frequency $8 \cdot 10^5$ Hz.

Y	PEO_1	PEO_2	PEO_3
0.02	0.053	0.200	0.205
0.05	0.070	0.218	0.221
0.10	0.257	0.507	0.536
0.12	0.260	0.578	0.694

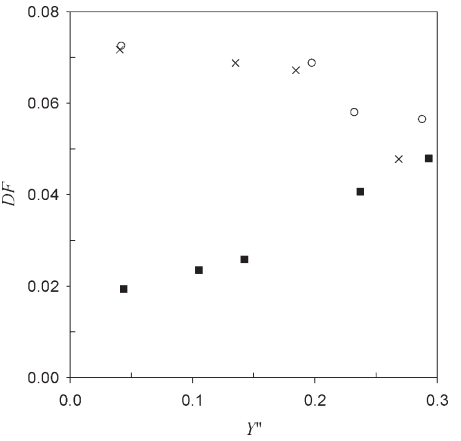

Figure 9.
Dissipation factor versus concentration Y''; ■ - PEO_1, ○ - PEO_2, × - PEO_3.

Results are depicted in Figure 9. We note, the dissipation factor slightly increases with salt content for the polymer with the lowest molecular mass and slightly decreases for polymers with higher molecular mass. They approach each other at high salt concentration.

Conclusion

The amorphous phase in polymer-salt solutions with low salt concentration rules dominantly ionic conductivity. In solutions comprising $LiClO_4$ and PEO samples of different molecular masses, composition of this phase can be determined from extent of crystallinity occurring in the systems. Moreover, melting point depression provides information about deviation of the solution from perfect behavior. It was found that ionic conductivity displays a power-law dependence on salt content of the amorphous phase. Ions are solvated by chain segments. The exponent reflects the extent of correlations between salt molecules and polymer segments. It results that exponent as well as mobility increase with molecular mass of PEO chains. The solution with the polymer of highest molecular mass behaves nearly perfectly. Moreover, it comprises the lowest mass fraction of crystalline phase. These facts favor ionic mobility. The probability of ion pair formation diminishes with increasing molecular mass. This is so

because this probability decreases with ascending exponent x as well as dielectric constant.

Acknowledgements: Fundamental Research Grant from Ministry of Higher Education, Malaysia, 600-IRDC/ST/FRGS.5/3/1144, supports this study.

[1] J. R. MacCallum, C. A. Vincent, Eds., "*Polymer Electrolyte Reviews - I*", Elsevier, London 1987.
[2] F. M. Gray, "*Polymer Electrolytes*", The Royal Society of Chemistry, Cambridge 1997.
[3] P. G. Bruce, "*Solid State Electrochemistry*", Cambridge University Press, Cambridge 1995.
[4] X. Qian, N. Gu, Z. Cheng, X. Yang, E. Wang, S. Dong, *Mat. Chem. and Phys.* **2002**, *74*, 98.
[5] S. J. Wen, T. J. Richardson, D. I. Ghantous, K. A. Striebel, P. N. Ross, E. J. Cairns, *J. Electroanalytical Chem.* **1996**, *408*, 113.
[6] R. Baskaran, S. Selvasekarapandian, N. Kuwata, J. Kawamura, T. Hattori, *Mat. Chem. and Phys.* **2006**, *98*, 55.
[7] V. Seneviratne, R. Frech, J. E. Furneaux, *Electrochimica Acta*, **2003**, *48*, 2221.
[8] B. Laik, L. Legrand, A. Chausse, R. Messina, *Electrochimica Acta*, **1998**, *44*, 773.
[9] M. B. Armand, J. M. Chabagno, N. J. Duclot, "*Fast Ion Transport in Solid*", P., Vashista, J. N., Mundy, G. K. Shenoy, Eds., Elsevier, North-Holland, Amsterdam 1979, p. 131.
[10] M. Jaipal Reddy, J. Siva Kumar, U. V. Subba Rao, Peter. P. Chu, *Solid State Ionics* **2006**, *177*, 253.
[11] E. A. Rietman, M. L. Kaplan, R. J. Kava, *Solid State Ionics* **1985**, *17*, 67.
[12] P. R. Sørensen, T. Jacobson, *Electrochimica Acta* **1982**, *27*, 1671.
[13] C. D. Robitaille, D. Fauteux, *J. Electrochem. Soc.* **1986**, *133*, 315.
[14] J. Li, E. A. Mintz, I. M. Khan, *Chem. Mater.* **1992**, *4*, 1131.
[15] J. R. Dygas, Z. Misztal-Faraj, Z. Florjańczyk, F. Krok, M. Marzantowicz, E. Zygadlo-Monikowska, *Solid State Ionics* **2003**, *157*, 249.
[16] S. L. Maunu, J. J. Lindberg, *Polym. Bulletin* **1987**, *17*, 545.
[17] W. Young, P. J. Brigandi, T. H. Epps, III, *Macromolecules* **2008**, *41*, 6276.
[18] Y. Zhao, R. Tao, T. Fujinami, *Electrochimica Acta* **2006**, *51*, 6451.
[19] L. A. Guilherme, R. S. Borges, E. M. S. Moraes, G. Goulart Silva, M. A. Pimenta, A. Marletta, R. A. Silva, *Electrochimica Acta* **2007**, *53*, 1503.
[20] C. H. Chan, H. W. Kammer, *J. Appl. Polym. Sci.* **2008**, *110*, 424.
[21] S. Cimmino, E. Di Pace, E. Martuscelli, C. Silvestre, *Makromol. Chem.* **1990**, *191*, 2447.
[22] M. J. O'Neil, *The Merck Index*, 14th Ed., Merck & Co. Inc., Whitehouse Station, NJ, USA 2006, p. 5539.
[23] D. R. Lide, "*CRC Handbook of Chemistry and Physics*", 87th Ed., Taylor & Francis, Boca Raton, London, New York 2006, p. 6–112.

